Chapter 1

Introduction

1.1 Spintronics

The advent of spintronic devices has marked a transformative era in data storage technology, offering innovative solutions to address the ever-increasing demands for higher storage capacity, faster data access, and reduced energy consumption. Spintronics, which harnesses the intrinsic spin of electrons in addition to their charge, has revolutionized the landscape of data storage (Elphick et al. (2021); Hirohata & Takanashi (2014); Puebla et al. (2020); Wollmann et al. (2014)). Traditional electronic devices rely solely on electron charge for information processing, limiting their potential in terms of speed and efficiency. In contrast, spintronic devices leverage the inherent "spin" of electrons, enabling the encoding of information as spin orientations. This groundbreaking approach not only overcomes the limitations of charge-based electronics but also paves the way for non-volatile, high-density, and ultra-fast data storage solutions. The evolution of spintronic devices for storage purposes has been driven by a relentless pursuit of new materials, advanced fabrication techniques, and novel device architectures, resulting in a paradigm shift that promises to redefine the future of data storage technology (Awschalom & Flatté (2007); Felser et al. (2007); Zhao & Prenat (2015)).

Heusler alloys (HAs) have emerged as pivotal materials in the realm of spintronics devices, playing a significant role in advancing the frontiers of information technology (Balke et al. (2008); Felser et al. (2007)). These compounds, with their diverse chemical compositions and versatile properties, are particularly appealing for spintronics applications. HAs exhibit a remarkable combination of half-metalicity, which means they possess a near-total spin polarization in their electronic structure, and they maintain both metallic and semiconducting characteristics. This unique attribute makes them ideal candidates for generating and manipulating spin-polarized currents, a fundamental requirement for efficient spintronic devices. HAs are used in spin valves, tunnel junctions, and spin filters, facilitating the efficient transport and manipulation of spin-polarized electrons. Their versatility and tunability, both in terms of composition and crystal structure, offer engineers and scientists the flexibility to design and optimize spintronics devices for diverse applications, including data storage, magnetic sensors, and spin-based logic devices. As the field of spintronics continues to advance, HAs remain at the forefront, demonstrating their pivotal role in enabling the development of next-generation, high-performance spintronic technologies.

1.2 Introduction to Heusler Alloys (HAs)

HAs was first discovered by Friedrich Heusler in 1903 and the first discovered system was Cu_2MnAl(Tavares et al. (2023)). This type of ternary alloy has been intensively investigated due to its ferromagnetism without containing any ferromagnetic elements, such as Fe, Co, Ni, and Gd. Typically, Heusler alloys are intermetallic compounds with the general formula XYZ, where X and Y are transition metals and Z is a main-group element (Graf et al. (2011)). The extensive array of potential constituents, as depicted in the colored periodic table figure 1.1, underscores the vast number of combinations possible. This abundance is reflected in the discovery of over 1000 Heusler compounds

to date. The classification of HAs is primarily based on the arrangement of atoms within their crystal structure and the specific combination of elements used in their composition. The classification encompasses a wide array of compositions, each with its own distinct electronic and magnetic characteristics, offering a rich landscape for both fundamental research and practical applications.

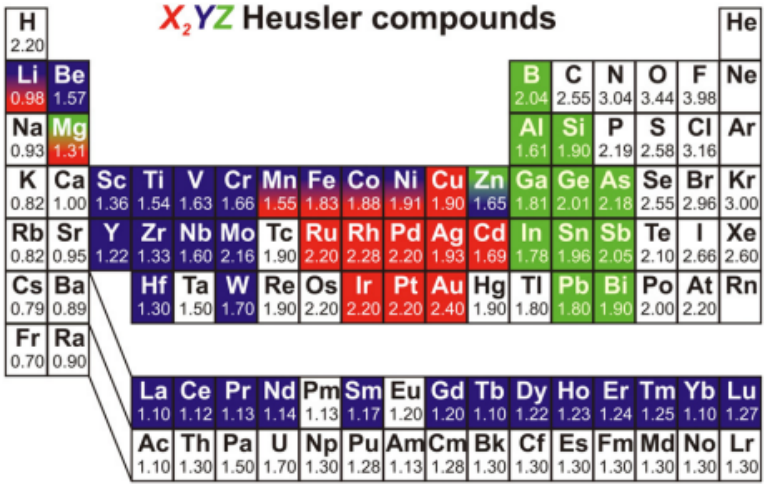

Fig. 1.1 Possible elements for the formation of Heulser alloys(Color coding indicates the choice for X,Y and Z elements).

Source:Graf et al. (2011)

1.3 Crystal structure and classification of HAs

There are two distinct families of HAs: one is Half Heusler XYZ with stoichiometry 1:1:1, and the other one is the full Heusler alloy X_2YZ with stoichiometry 2:1:1. Presently researchers are also exploring another type which is quaternary Heusler alloys, $XX'YZ$ with a stoichiometry of 1:1:1:1. Generally these compounds crystallizes in the $L2_1$ structure with space group $F\bar{4}3m$ as shown in figure 1.2

1.3.1 Full Heusler alloy

The X_2YZ structure comprises four interpenetrating face-centered cubics (fcc) sublattices. Notably, two of these sublattices are equally occupied by X atoms. In the $L2_1$ structure, X atoms are positioned at the 8c Wyckoff site (1/4, 1/4, 1/4), while the Y and Z atoms are situated at the 4a (0, 0, 0) and 4b (1/2, 1/2, 1/2) Wyckoff positions, respectively as shown in figure 1.2 (a). Sometimes, the standard $L2_1$ structure gets distorted due to mutual changes in the atomic positions of the elements. There are several kinds of disorders that are possible in HAs (Felser & Hirohata (2015)). In the B2 type, the disorder is in between the Y and Z atoms; hence, the 4a and 4b positions become equivalent in this type. Now, the space group is also changed from the ordered $Fm\bar{3}m$ to $Pm\bar{3}m$. In A2 type disorder all the elements X, Y, and Z are randomly taken the Wykoff positions as shown in figure 1.2 (c). The most commonly observed disorder is B2 type disorder. To identify these disorders, the most prominent technique is synchrotron X-ray diffraction (XRD)(Takamura et al. (2010)). In the case of the ordered structure, both fcc reflections (111) and (200) are observed. But, if a system has a B2 type disorder, then (111) peak disappears from the XRD pattern. In A2 type disorder, both the reflections (111) and (200) are not visible. The presence of disorders in the system adds complexity to the system, but it also gives rise to numerous advantageous phenomena[Graf et al. (2011)].

1.3.2 Equiatomic quarternary Heusler alloy(EQHAs)

In full Heusler alloys, if one of the X atoms is switched out for a different transition element, the new alloy is called a quaternary or equiatomic quaternary Heusler alloy and has the formula $XX'YZ$ (Gupta et al. (2021)). In this case, the crystal structure is $LiMgPdSn$, which is a Y-type structure with the space group $F\bar{4}3m$. Like Full HAs, QHAs crystal structure comprises four interpenetrating face-centered cubic (FCC) sublattices. Notably, here two different X atoms occupied the 4a (0, 0, 0) and 4d (3/4, 3/4, 3/4) Wyckoff

sites, respectively. The *Y* atom placed at 4b (1/2, 1/2, 1/2) and Z atom is placed at 4c (1/4, 1/4, 1/4) as shown in figure 1.2 (d).

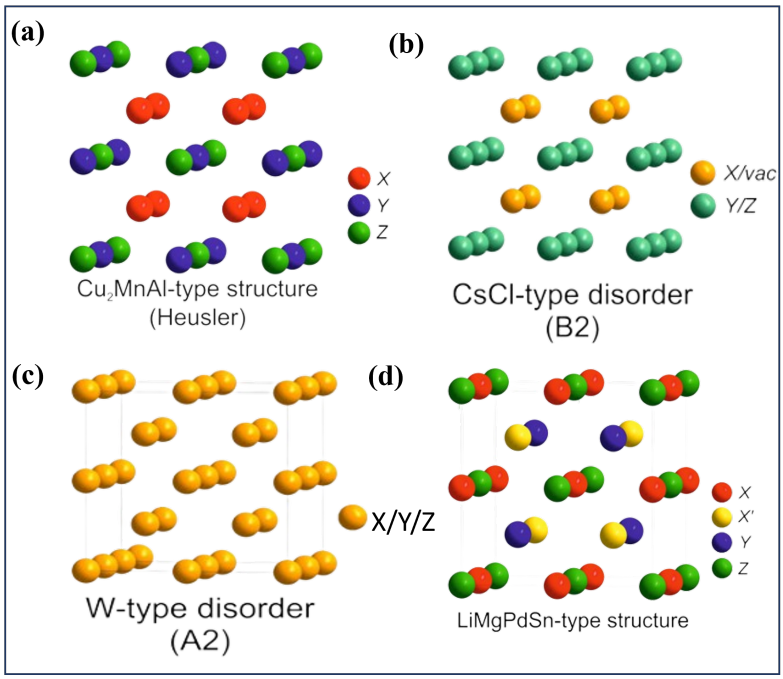

Fig. 1.2 The unit cell structure of ordered full Heusler alloy (a), unit cell structure with B2 and A2 disorder (b and c respectively.) and quaternary Heusler alloy (d)

Source:Graf et al. (2011)

1.4 Magnetism in Heusler alloys

The first discovered compound was Cu_2MnAl is ferromagnetic, while none of the constituents have a magnetic nature. The origin of magnetism in Heusler alloys, despite the constituent elements not being inherently magnetic, can be attributed to the unique electronic structure and specific arrangement of atoms within the alloy's crystal lattice (Kurt et al. (2016)). The magnetic properties of Heusler alloys arise from the interaction between the electronic states of different elements in the compound. HAs often exhibit a variety of magnetic behaviors, including ferromagnetism, antiferromagnetism, or even ferrimagnetism (Benea et al. (2019); Elphick et al. (2021)).

The key factor is the presence of localized magnetic moments associated with certain atoms, typically transition metal atoms, within the crystal structure (Kulkova et al. (2006)). The interaction between these magnetic moments gives rise to the overall magnetic behavior of the alloy.

In some Heusler alloys, the arrangement allows for the alignment of magnetic moments, leading to ferromagnetism, where the magnetic moments of adjacent atoms align parallel to each other. In other cases, the arrangement may favor antiferromagnetic coupling, where adjacent magnetic moments align in opposite directions, resulting in a cancellation of overall magnetic moments. The intricate interplay of these interactions, along with the electronic band structure of the alloy, determines the magnetic characteristics observed.

1.4.1 A brief introduction to magnetism

on the specific combination of elements and their ordering, Heusler alloys can exhibit ferromagnetic, antiferromagnetic, ferrimagnetic behavior, or spin glass behavior, making them highly adaptable for applications in spintronics, magnetocaloric devices, and other advanced technologies [Willoughby et al. (2015)].

- **Ferromagnetic Materials (FM) :** FM materials generate a robust and macroscopic magnetic field through the spontaneous alignment of the magnetic moments of individual atoms or ions in the same direction as depicted in figure 1.3. Furthermore, FM materials (Blundell (2001)) retain their magnetization even after the applied magnetic field is removed, as a result of an intrinsic property they possess. The generation of magnetic domains is a consequence of FM materials effectively reducing the free energy of the system. When no magnetic field was present, these magnetic domains aligned at random in FM materials. On the contrary, when a magnetic field is applied, all magnetic moments align parallel to one another in the same direction. Furthermore, even after the magnetic field is removed, certain

domains continue to predominate in the same direction, resulting in the formation of remanent magnetization.

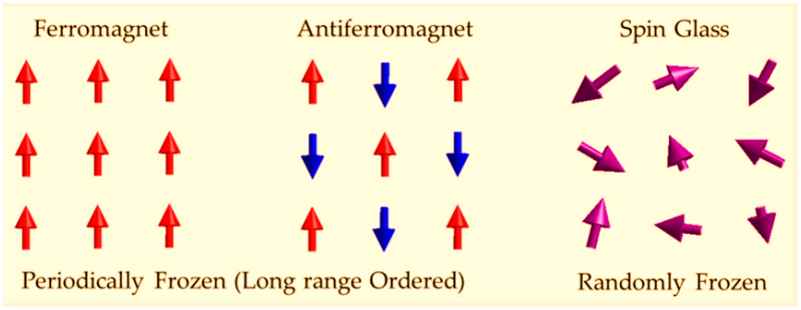

Fig. 1.3 Spin alignment of a ferromagnetic, antiferromagnetic, and spin glass system.

Source: Sato et. al. Symmetry 2020, 12, 1910

- **Antiferromagntic Materials (AFM):** AFM materials are characterized by the cancellation of their overall magnetic moment due to the alignment of adjacent magnetic moments in opposite orientations as shown in figure 1.3. While these substances may demonstrate atomic-level magnetic behavior, their overall magnetic impact is frequently insignificant.

- **Spin glass (SG) :** Spin glasses are characterized by the random freezing of magnetic spins below a specific temperature known as the spin-glass blocking temperature (T_f) as shown in figure 1.3. The very first evidence of the spin-glass transition occurred in metallic alloy systems comprising magnetic ions with low concentrations, such as CuMn, AuFe, AgMn, and so forth Binder & Young (1986); da Silva Jr et al. (2019). Magnetic systems that experience frustration, disorder, and randomness can result in a state known as spin-glass.

1.4.2 Origin of Spin Frustration

Spin glass, an emerging and captivating realm within the field of magnetism, stands in stark contrast to conventional long-range ordered magnetic states (Campbell & Bernardi

(1995); Goremychkin et al. (2008); Krusin-Elbaum et al. (1983)) as mentioned in figure 1.3. Instead, it exhibits a collective nature during its low-temperature phase, reminiscent of the characteristics observed in normal glass. Much like the subtle flow of structural glasses, the spins in this magnetic state appear to adopt a seemingly random orientation, yet they remain unchanging over time. This peculiar magnetic phase derives its name from the close resemblance to the frozen random orientation of particles in ordinary glasses, thus coining the term "spin glass."

The existence of the glassy phase in spin glasses can be attributed to three fundamental factors: *randomness, mixed interactions, and frustration.* The disorder or randomness in spin glasses arises from the randomization of distances between magnetic moments, referred to as site randomness, or from nearest neighbor interactions in a regular lattice, known as bond randomness. Additionally, these interactions must exhibit randomness in strength, coupled with a blend of ferromagnetic (FM) and antiferromagnetic (AFM) natures. This intricate interplay of randomness and competing interactions gives rise to frustration. To Understand this, let's take an example of a triangular lattice. In figure1.4, we are presented with a tangible example illustrating the concept of frustration. Consider three spins situated at the vertices of a triangular lattice. Each spin is exclusively connected to its two neighboring spins, with the nature of their interaction depicted by arrow signs along the edges. In cases where the interaction is antiferromagnetic, the spins tend to align in an anti-parallel direction. As illustrated in figure1.4, the interaction between the top and left basal spin is antiferromagnetic, leading the left basal spin to adopt a downward orientation ($\downarrow$) to align with this coupling.

However, attention is drawn to the right basal spin, denoted by a question mark. This spin encounters a decision-making dilemma, forced to determine its orientation. If it prioritizes coupling with the top spin, it should point downward ($\downarrow$); if it considers interaction with the left basal spin, it should point upward ($\uparrow$). Consequently, the spin

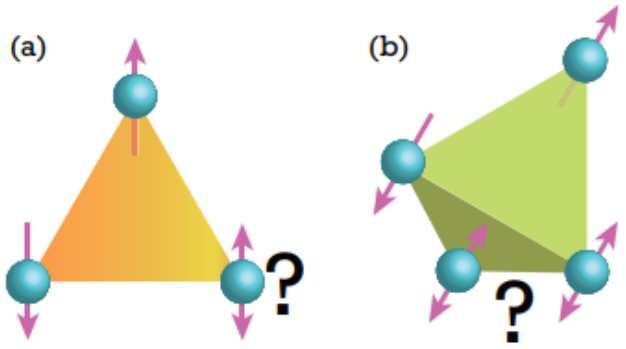

Fig. 1.4 Illustration of a 2D triangular lattice and tetrahedral lattice with geometric spin frustration, where not all nearest neighbor antiferromagnetic interactions can be satisfied simultaneously.

finds itself unable to simultaneously satisfy both couplings, giving rise to what is aptly termed "frustration." The same phenomenon is also evident in a tetrahedral lattice structure, as depicted in figure1.4. spin frustration leads to different magnetic phenomena, viz. low-temperature spin glass or re-entrant spin glass or cluster glass (CG), exchange bias (EB), magnetic memory effect, etc. The CG phenomenon occurs in a system where one of the competing interactions between ferromagnetism (FM) and antiferromagnetism (AFM) prevails over the other. Notably, the cluster of spins forms a larger entity compared to individual atomic spins, presenting itself as a substantial spin moment. The preliminary exploration of the characteristics of glassy behavior is conducted through diverse models employing frequency-dependent alternating current (ac) susceptibility measurements, as outlined below

- **Vogel-Fulcher Model:** The Vogel-Fulcher Model plays a pivotal role in comprehending glassy behavior, offering insights through the analysis of peak temperatures at various frequencies. This empirical law delves into the viscosity of supercooled liquids, expressing it through the formula;

$$\tau = \tau_0 \exp\left(\frac{E_A}{K_B(T_f - T_{SG}}\right) \tag{1.1}$$

Here, the parameters τ_o, E_A, and T_{SG} are determined through fitting, with T_{SG} referred to as the spin glass temperature. Unlike a simple activation fit, this model provides more plausible physical parameters.

- **Dynamic-Scaling Model:** The standard theory of dynamic scaling is applied in the vicinity of a phase transition temperature. The implications of dynamic scaling establish a connection between the critical relaxation time τ and the standard correlation length ζ, expressed as $\zeta \sim \tau^2$. Thus, power-law divergence takes the form:

$$\tau = \tau_0 \left(\frac{T_f}{T_{SG}} - 1 \right)^{-z\nu} \tag{1.2}$$

where τ is the relaxation time ($\tau = 1/2\pi f$), T_{SG} is the freezing temperature of spins, z is the dynamic critical exponent, and ν is the critical exponent of the correlation length. $z\nu$ is the dynamical critical exponent, which should be between 4 to 12 for glassy transition Further substantiating the delayed spin relaxation in the Spin Glass (SG) or Cluster Glass (CG) phase involves examining the time-dependent measurements of thermo-remanent magnetization $m(t)$ within the SG/CG region—specifically, below the freezing transition temperature T_f. This experimental data can be effectively modeled and fitted by the following expression:

- **KWW Model:** The KWW (Kohlrausch Williams Watt) model, initially introduced by R. Kohlrausch in 1854 to analyze the charge of the capacitor (Leyden jar), has evolved over time. Williams and D. C. Watts later introduced the Fourier transform of the stretched exponential in 1970, focusing on the dielectric spectra of polymers. This stretched exponential relaxation has empirically manifested in various amorphous materials, including polymers, glasses, and glass-forming liquids near the glass transition temperature.

The versatility of the KWW function is reflected in its widespread application for analyzing relaxations of various natures, such as viscosity, friction, gas kinetics, heat transfer, and more. In the context of this study, the Thermo-Remanent Magnetization (TRM) measurement was conducted using the field-cooled protocol. This involves cooling the sample under the application of a magnetic field to the desired temperature, followed by measuring time-dependent magnetization data after completely removing the magnetic field. The $m(t)$ has been plotted against time, and the time evolution of TRM is scrutinized using the KWW stretched exponential equation as follows.

$$m(t) = m_0 - m_g \exp\left\{\left(-\frac{t}{\tau}\right)^{\beta}\right\} \tag{1.3}$$

In this equation, m_0 represents the initial remanent magnetization, m_g signifies the magnetization of the glassy component, τ is the characteristic relaxation time constant, and β serves as the shape parameter or stretching exponent. The β value, ranging from 0 to 1, provides insights into the disordered nature of various systems.

1.4.3 Exchange Bias (EB) :

Exchange bias (EB) stands as an intriguing phenomenon situated at the crossroads of magnetism and materials science, captivating researchers for several decades (Morales et al. (2015)). It arises from the complex interplay between ferromagnetic (FM) and antiferromagnetic (AFM) materials, marked by a distinctive shift in the magnetization vs. field curve, introducing unidirectional anisotropy to the system as shown in figure 1.5. Meiklejohn (Meiklejohn & Bean (1956)) and Bean initially reported this phenomenon in 1956 while studying cobalt particles within their parent AFM oxide (Punnoose et al. (2001)). FM systems exhibit spontaneous magnetization even without a magnetic field, while AFM materials have negative nearest-neighbor exchange interactions. Magnetic properties are described through hysteresis loops and susceptibility data, with EB field (H_E)

and coercivity (H_C) estimated as $H_E = |H_{C1} + H_{C2}|/2$ and $H_C = |H_{C1} - H_{C2}|/2$, where H_{C1} and H_{C2} are the left and right coercive field values. The EB phenomenon is explained as follows: When a magnetic field is applied at temperatures between T_N and T_C, the EB effect emerges due to the coupling of the FM and AFM layers. Initially, AFM spins are randomly distributed in their paramagnetic state, while FM spins align with the applied field (stage 1). As the sample cools below T_N, the AFM spins at the interface coupled with FM spins, leading to their alignment along the magnetic field direction (stage 2). Uncompensated spins at the interface result in a nonzero magnetization at the monolayer (Nayak et al. (2015)).

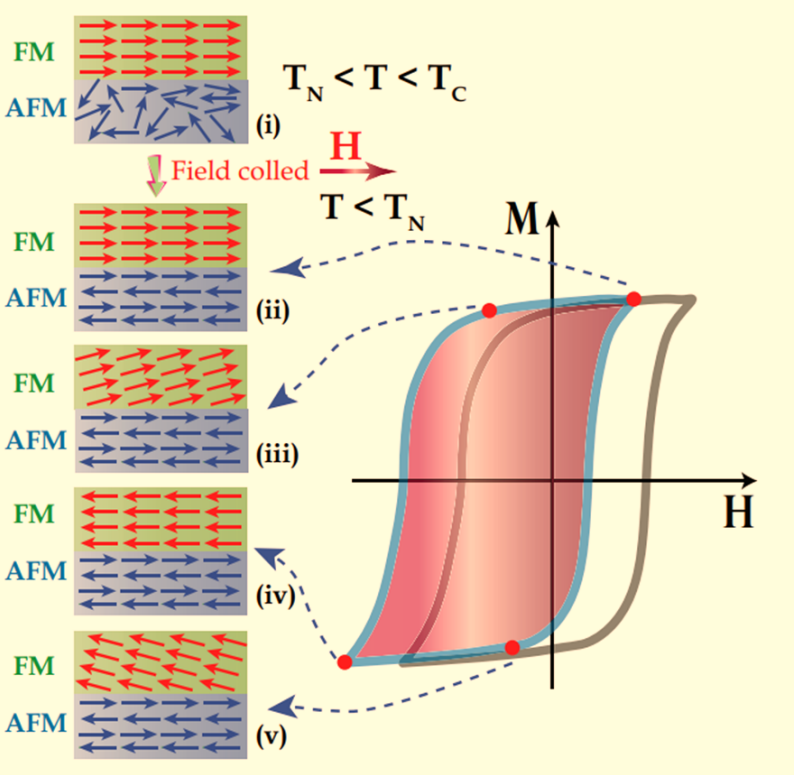

Fig. 1.5 Schematic representation of exchange bias effect.

During a reversal of the magnetic field, FM spins rotate, but AFM spins at the interface remain unchanged due to large AFM anisotropy (stage 3). A microscopic torque is generated at the interface by AFM spins on FM spins, requiring additional field strength to

reverse the FM layer completely (stage 4). Upon rotation of this field back to its original direction, FM spins initiate rotation at a smaller field strength due to the alignment of the microscopic torque in the same direction as the field (stage 5). This results in a shift of the hysteresis loop along the field axis, known as EB.

1.4.4 Magnetic memory effect

This effect is frequently associated with the capacity of a material to "remember" or retain its magnetic properties when exposed to an external magnetic field in the context of magnetism and magnetic materials. The development of magnetic storage and memory devices, including magnetic random-access memory (MRAM) and other types of non-volatile memory, is significantly influenced by this phenomenon. Memory effects are commonly observed in systems with strong frustration, particularly below their freezing points. As reported in the case of nanoparticles, their blocking temperature was determined to be 78 K. Consequently, the memory effect was observed below this critical blocking temperature, as illustrated in the accompanying figure 1.6 (Sun et al. (2003))

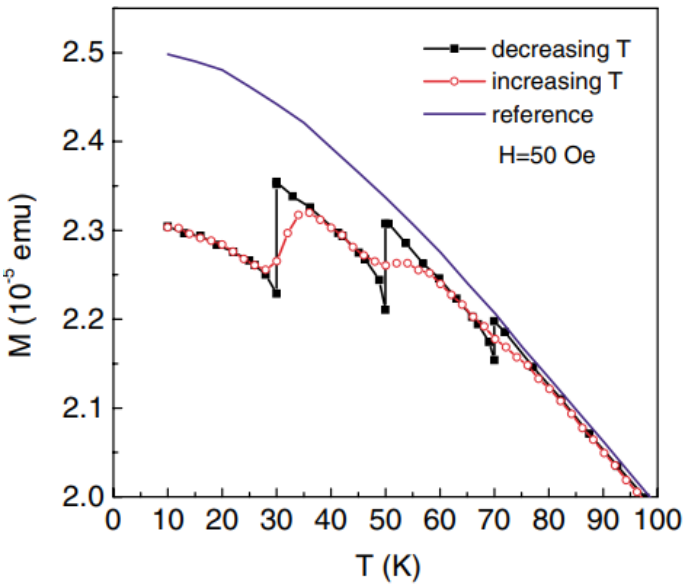

Fig. 1.6 The memory effect in the DC magnetization is evident in the presented data 1.6

1.5 Transport properties

1.5.1 Longitudnal Resistivity

Electrical resistivity is a characteristic of materials that tells us how well a material can conduct or hinder the flow of electric current. It is influenced by external factors like temperature, magnetic field, doping, and pressure. In metals and alloys, resistivity is a result of charge carriers being scattered by various elements like phonons, magnons, and defects. Matthiessen's rule states that the overall resistivity can be expressed as the sum of these scattering effects

$$\rho(T) = \rho_0 + \rho_{(ph)}(T) + \rho_{mag}(T) \tag{1.4}$$

The term ρ_0 represents the residual resistivity, which remains constant regardless of temperature and arises from the scattering of charge carriers by defects. The resistivity denoted by $\rho_{(ph)}$ is caused by the scattering of charge carriers due to phonons and is calculated using the formula provided below

$$\rho_{(ph)}(T) = 4R\left(\frac{T}{\theta_D}\right)^5 \int_0^{\frac{T}{\theta_D}} \frac{x^5}{(1-e^{-x})(e^{-x}-1)} dx \tag{1.5}$$

Here, R is the gas constant. The phonon vibrations in a crystal have a characteristic temperature, θ_D the Debye temperature. When $T > \theta_D$, the amount of electron-phonon scattering increases in a linear fashion with T. Below θ_D electron-phonon scattering varies proportionately to T^3, and at very low temperatures $T < \theta_D$, it shows a T^5 dependency referred known as the Bloch Law. Magnons, which are quantized spin waves comparable to phonons, contribute to the resistivity with a quadratic temperature dependency arising from magnon scattering.

1.5.2 Magnetoresistance (MR)

The resistance of the material, when measured under the applied external magnetic field is called magnetoresistance (MR).

1.5.3 Hall Effect

1.5.4 Normal Hall effect

In 1879, Edwin Hall made a significant discovery known as the Hall effect. This phenomenon involves the generation of a voltage difference, called the Hall voltage, across an electrical conductor (Nagaosa et al. (2010)). This voltage occurs perpendicular to both the electric current flowing through the conductor and a magnetic field applied to it, as illustrated in figure 1.7. As shown in figure 1.7, the magnetic field (B) is applied perpendicular to the current (I), the charge carriers (such as electrons, holes, or ions) experience the Lorentz force following equation:

$$F = q[E + (v \times B)] \tag{1.6}$$

This force causes their paths to curve, unlike the straight paths they would follow in the absence of a magnetic field. As a result, charge carriers accumulate on one face of the conductor, while equal and opposite charges build up on the other face. This charge separation generates a transverse voltage known as Hall voltage (V_H) and the associated resistivity is known as Hall resistivity $(\rho_{xy} = R_o H)$. Here, R_0 is the ordinary Hall coefficient. The Hall field opposes the further movement of charges, creating a steady electric potential as long as the charge continues to flow. The Hall field grows until it counteracts the Lorentz force entirely. In the steady-state condition, the magnetic force on each charge carrier in the y direction is balanced by an electrical force along the y-axis due

to the accumulation of charges, as shown in figure1.7. Consequently, charge carriers do not move in the y direction. Thus, in a steady state,

$$V_H = v_x B_z d = \frac{I_x B_z}{nte} \tag{1.7}$$

Here, t is the thickness of the system, and n is the carrier concentration. Hence, the Hall coefficient is given by:

$$R_H = \frac{V_H t}{IB} = -\frac{1}{ne} \tag{1.8}$$

In order to determine the concentration and type of current carrier (electrons or holes) in a system, it is necessary to measure the Hall effect. A positive Hall coefficient is shown if holes are the major carriers. However, a negative Hall coefficient is seen when electrons are the predominant carrier.

1.5.5 Anomalous Hall effect

After the discovery of the normal Hall effect, Subsequently, Edwin H. Hall made the observation that the precession of electrons in the ferromagnetic (FM) conductor was ten times more intense than in the nonmagnetic conductor (Nagaosa et al. (2010)). This was termed as anomalous Hall effect (AHE). Now the total Hall resistivity is expressed as the sum of ordinary Hall resistivity $(R_0 H)$ and the anomalous Hall resistivity$(R_s M)$; (Jungwirth et al. (2002); Tian et al. (2009)), i.e.,

$$\rho_{xy} = R_0 H + R_s M \tag{1.9}$$

Here, R_s and M are anomalous Hall coefficient and magnetization of the system, respectively (Nagaosa et al. (2010)).

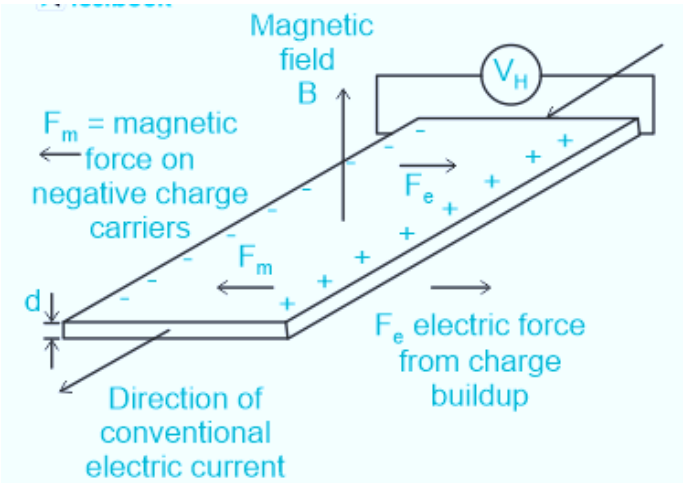

Fig. 1.7 Geometrical representation of ordinary Hall effect

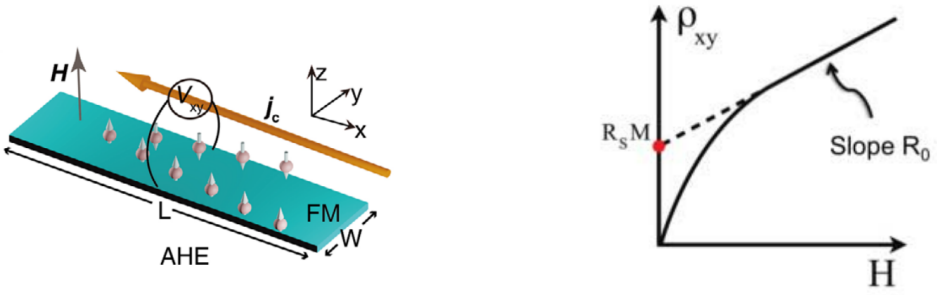

(a) (b)

Fig. 1.8 (a) Geometrical representation of anomalous Hall effect (b) The Hall resistivity (ρ_{xy}) Vs. the magnetic field of a ferromagnetic conductor, here R_SM denotes the zero-field intercept associated with the AHE as mentioned in equation 1.9

An illustration of the anomalous Hall effect and the field-dependent variation of ρ_{xy} is presented in figure 1.8. Evidently, as shown in figure 1.8, ρ_{xy} increases initially in response to the applied field. However, beyond a certain field, it tends to saturate in a manner similar to magnetization, as the second term in equation 1.9 represents AHE. In contrast, the first term in equation 1.9 continues to increase in magnitude with the applied field.

Initially, it was believed that the increase in the magnitude of ρ_{xy} was due to magnetization, which adds more precession of electrons in the system, but later it was found that there are basically two: (i) intrinsic and (ii) extrinsic mechanisms that are responsible for the AHE.

- **Intrinsic deflection:** Intrinsic deflection is independent of the scattering mechanism. The theory of intrinsic deflection was proposed by Karplus and Luttinger in 1954 (Karplus & Luttinger (1954)). This mechanism is intricately linked to the electronic band structure of materials. The Berry curvature functions like a pseudomagnetic field within momentum space. This pseudo-magnetic field imparts an unusual velocity to conducting electrons, causing them to move perpendicular to the applied electric field as shown in figure **??** (a). Notably, this phenomenon gives rise to the AHE, even when there is no external magnetic field present. (Rout et al. (2019))

- **Extrinsics Mechanism:** The external mechanisms are usually linked to the scattering of conduction electrons by impurities, defects, or irregularities within the material. They play a crucial role in altering the expected trajectories of electrons, deviating from the classical Hall effect figure **??** (b,c). This alteration leads to the manifestation of the anomalous Hall voltage. Both skew scattering and the side jump effect fall under the category of extrinsic mechanisms, and they are particularly influenced by scattering events. These mechanisms arise from the interactions between conduction electrons and magnetic impurities present in ferromagnetic (FM) materials.

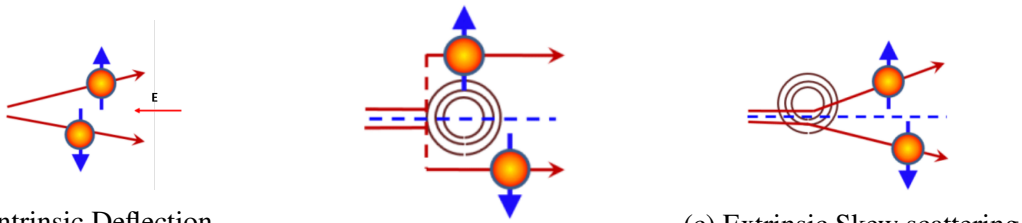

(a) Intrinsic Deflection (b) Side jump (c) Extrinsic Skew scattering

Fig. 1.9 Schematic representation of the major mechanisms

1.6 Outlines of the thesis

The primary objective of this thesis is to uncover innovative multifunctional materials within the Heusler family, including both full and Quarternary Heusler compounds, by conducting a comprehensive analysis of the magneto-transport property relationships. This exploration involves the introduction of novel substitutions, notably the Co element. Furthermore, we have undertaken microstructural investigations to elucidate the underlying mechanisms behind magnetostructural transitions in certain cases. This research is anticipated to yield the discovery of novel materials with significant potential for practical applications. Additionally, it is expected to contribute valuable insights into the fundamental principles governing the physics of magnetism in Heusler alloys more broadly. The core focus of my research centers around the investigation of Co-doped full and quaternary Heusler alloys, which are renowned for their exceptional attributes, including a high Curie temperature and significant spin polarization. By delving into the magnetic and transport properties of these Heusler systems, I aim to unlock their potential for diverse applications. Additionally, our exploration extends to Ni-based full Heusler alloys, where we have uncovered intriguing phenomena such as antisite disorder and structural alterations. The presence of these structural changes within the system has yielded intriguing effects, notably manifesting as asymmetry in magnetoresistance. These findings serve as compelling motivation for the pursuit of deeper insights into the unique characteristics and potential applications of these materials in my thesis. In addition to our extensive investigation of Co-doped Heusler alloys and Ni-based full Heusler systems, our research endeavors are motivated by the quest to unearth materials with ideal attributes for thermoelectric applications. The pursuit of high thermoelectric efficiency necessitates the discovery of materials with a remarkably high Seebeck coefficient. In this vein, our exploration extends to evaluating the thermoelectric properties of these systems. What makes our study even more intriguing is the rare and fascinating phenomenon we've uncovered: a pronounced

decoupling between the Seebeck coefficient (S) and the electrical conductivity (σ) within a specific temperature range. Such a decoupling is a rarity in material systems and holds the potential to revolutionize the field of thermoelectric materials. The interplay of these remarkable properties with the other characteristics of our Heusler alloys underscores the multifaceted nature of our research, making it a captivating and promising endeavor in the realm of materials science.